Trop J Nat Prod Res, June 2023; 7(6):3158-3167 ISSN 2616-0684 (Print)
ISSN 2616-0692 (Electronic)

Tropical Journal of Natural Product Research

Available online at https://www.tjnpr.org

Original Research Article

Synthesis, Anti-breast Cancer Activity, and Molecular Docking Studies of Thiourea Benzamide Derivatives and Their Complexes with Copper Ion

Yaqeen M. Al-Salim and Rafid H. Al-Asadi*

Department of Chemistry, College of Education for Pure Sciences, University of Basrah, Basrah, 61004, Iraq.

ARTICLE INFO

Article history:
Received 14 April 2023
Revised 10 June 2023
Accepted 14 June 2023
Published online 01 July 2023

ABSTRACT

Recently, there has been a rise in interest in the synthesis of chemical compounds with biological activity, especially in the fight against cancer, which is regarded as a modern-day disease. The present study was conducted to synthesize thiourea benzamide derivative ligands and their metal complexes with Cu(II). Thiourea benzamide derivative ligands and their metal complexes with Cu(II) were synthesized. The structures of the synthesized complexes were elucidated by mass spectra, FT-IR, ^{13}C-NMR, and ^{1}H-NMR spectra. Molar conductivity, magnetic susceptibility, SEM, EDX, and TG analyses were also performed. The *in vitro* anticancer activity of the compounds was examined against the breast cancer cell line MCF-7. Molecular docking of complexes (1) and (2) was performed with breast cancer proteins. The synthesized compounds include {[Cu(L)$_2$Cl$_2$].nH$_2$O, where L= (N-((3-nitrophenyl) carbamothioyl) benzamide (L1, n= 2, (1)), N-(naphthalen-1-ylcarbamothioyl) benzamide (L2, n= 2, (2)), 4-nitro-N-((4-nitrophenyl) carbamothioyl) benzamide (L3, n= 0, (3)), 4-nitro-N-(p-tolylcarbamothioyl) benzamide (L4, n= 2, (4)), N-((4-chlorophenyl) carbamothioyl)-4-nitrobenzamide (L5, n= 4, (5). The ligands behave as bidentate donors and are associated with Cu(II) in a 1:2 (M:L) ratio. Also, the geometric shapes of the prepared complexes were octahedral. The *in vitro* cellular toxicity evaluation showed that the compounds have low efficacy except for complexes (1) and (2), which have high effectiveness. The molecular docking analysis indicated that the compounds would specifically target PR (PDP: 4OAR) and Akt (PDP: 5KCV) proteins, which had the lowest values of binding energy and RMSD. The findings of this study reveal that these compounds can be used for therapeutic purposes.

***Keywords*:** Breast cancer, Metal complexes, Molecular docking, MTT, SEM, Thiourea benzamide.

Introduction

Thioureas are a well-known class of versatile organic compounds that have been extensively synthesized and investigated for many years due to their ability to undergo structural modification.[1] These compounds have proven to be industrially important by having two reactive primary amine group units. Thiourea can therefore be used to create a wide range of useful biologically interesting chemical groups, leading to an essentially infinite number of structures with novel physicochemical features. These properties add to the understanding of thiourea chemicals.[2-4] Compounds containing carbonyl and thiocarbonyl groups occupy a necessary position among organic reagents as workable donor ligands for transition metal ions. [5-6] Among these thiourea derivatives are potentially very versatile ligands and can coordinate to a range of metal centers as neutral ligands, monoanions, or dianions.[6-7]

A wide range of thiourea applications in industries, chemistry, medicine, and other fields may be facilitated by the oxygen, nitrogen, and sulphur donor atoms of thiourea and its derivatives.

*Corresponding author. E mail: dr.rafid74@yahoo.com
Tel: +9647712549614

Citation: Al-Salim YM and Al-Asadi RH. Synthesis, Anti-breast Cancer Activity, and Molecular Docking Studies of Thiourea Benzamide Derivatives and Their Complexes with Copper Ion. Trop J Nat Prod Res. 2023; 7(6): 3158-3167 http://www.doi.org/10.26538/tjnpr/v7i6.15

Official Journal of Natural Product Research Group, Faculty of Pharmacy, University of Benin, Benin City, Nigeria.

The ligands and their metal complexes also exhibit a wide spectrum of biological action, acting as anticancer, antioxidant, anti-HIV, anti-parasitic, anti-inflammatory, fungicide, herbicide, antiviral, rodenticide, and plant growth regulators.[8-11] Thiourea derivatives may have mono, binary, triple, or quadruple substituents depending on the extent of substitution on nitrogen atoms. One of the most important types of thiourea derivatives that have been studied recently is carbonyl thiourea, which has the following general formula.[12]

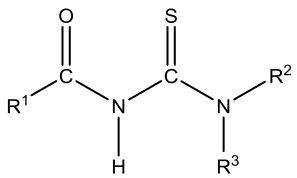

Where the R^1, R^2, and R^3 groups are H, alkyl, aryl, or heterocyclic rings.

Thiourea molecules and their derivatives can form coordination bonds with metal ions through the two nitrogen atoms in addition to the sulfur atom.[13] It was found that the metal ion plays an important role in determining the atom that donates electrons. As for complexes of transitional elements, coordination is often carried out through the sulfur atom.[14] The majority of these complexes are octahedral, except the copper element, which takes the form of a tetrahedron, according to research on the stereographic shapes of numerous complexes produced by the interaction of thiourea derivatives and some first transition series elements.[15,16]

The present study was aimed at synthesizing five compounds of thiourea benzamide derivatives (L1, L2, L3, L4, and L5) and their metal complexes [(1), (2), (3), (4), and (5)] with Cu(II), respectively. The *in*

vitro biological activity of prepared compounds as anti-breast cancer agents against the MCF-7 cell line was also evaluated.

Materials and Methods

Materials used

Benzoyl chloride, 4-nitro benzoyl chloride, ammonium thiocyanate, 1-naphthylamine, 3-nitroaniline, 4-nitroaniline, 4-methylaniline, 4-chloroaniline, hydrated copper chloride ($CuCl_2.2H_2O$), ethanol, methanol, acetone, chloroform, ethyl acetate, hexane, and diethyl ether were purchased from Sigma-Aldrich and Merck. All chemicals were of a high degree of purity (~97-99 %).

Equipment used

The melting point of compounds was measured by (Thermo Scientific) apparatus. FT-IR spectra were recorded using KBr on (FT-IR-84005-SHIMADZU, Japan) in the range of (400–4000 cm^{-1}). ^1H and ^{13}C-NMR spectra of the ligands were recorded on a spectrometer (Bruker- 400Hz) by using tetramethylsilane (TMS) as an internal standard and deuterated chloroform solvent. The EI-MS for ligands was examined on a spectrometer (Agilent Technologies 5975C, USA) while ESI-MS for complexes was recorded on Shimadzu LCMS (2010A, Japan). The molar conductivity measurements of complexes were measured by using HI 2315 conductivity meter (Romania) in DMSO with a concentration of 10^{-3}M at room temperature (25-35ºC). Magnetic susceptibilities of complexes were recorded by using the auto magnetic susceptibility balance (Sherwood Company, Germany). Thermo-gravimetric analysis (TGA) of complexes was performed by a device (Build 20 SDT Q600 V20.9) of American origin. Field emission scanning electron microscopy (FESEM) and energy-dispersive X-ray spectroscopy (EDX) were measured for some compounds prepared using a German-made device (Sigma VP Model-ZEISS Company).

Synthesis of the ligands

N-([3-nitrophenyl] carbamothioyl) benzamide (L1)

A solution (10 mmol) containing 1.41 g of benzoyl chloride in 15 mL of acetone was added progressively to a solution containing 0.67 g of ammonium thiocyanate in 10 mL of acetone (10 mmol). The mixture was refluxed for 1 h with stirring, and the product was filtered, then added while hot to a solution that was made from 1.38 g of 3-nitroaniline in 20 mL acetone (10 mmol). The mixture was refluxed with a stirrer for 6 h, and followed by thin layer chromatographic (TLC) analysis (ethyl acetate: hexane, 3:7). The yield was cooled, filtered, dried, and recrystallized using hot absolute ethanol. The product was white. Yield: 52.09%, m.p.: 159–161 °C. IR spectrum, ν, cm^{-1}: 3244 (N–H), 3097 (Ar–CH), 1668 (C=O), 1600 (C=C), 1529 and 1344 (NO_2), 1159 (C=S). ^1H NMR spectrum, δ, ppm: 7.62-7.60 m (3H, Ar–Hi+Hi'+Hj), 7.70 t (1H, Ar–Hg), 7.90 d (2H, Ar–Hf+Hf'), 8.06 d (1H, Ar–He), 8.13 d (1H, Ar–Hd), 8.80 s (1H, Ar–Hc), 9.20 s (1H, NHa), 12.90 s (1H, NHb). MS (EI, m/z (%)): 301.1[M^+, 20.4].

N-(naphthalen-1-ylcarbamothioyl) benzamide (L2)

A similar procedure was used as in L1, except instead of 3-nitro aniline, 1.43 g of 1-naphthyl amine (10 mmol) was employed. The product was a greenish yellow. Yield: 40.14 %, mp: 167–168 °C. IR spectrum, ν, cm^{-1}: 3317 (N–H), 3016 (Ar–CH), 1672 (C=O), 1629 (C=C), 1525 and 1346 (NO_2), 1147 (C=S). ^1H NMR spectrum, δ, ppm: 7.52-7.69 m (5H, Ar–H), 7.70 t (1H, Ar–Hf), 7.87 d (1H, Ar–Hg'), 7.91 d (1H, Ar–Hg), 7.97 d (2H, Ar–Hd+Hd'), 8.03 d (2H, Ar–Hc+Hc'), 9.28 s (1H, NHa), 12.76 s (1H, NHb). ^{13}C NMR spectrum, δ_C, ppm: 180.09(C_1), 167.24(C_2), 134.20(C_3), 133.90(C_4), 133.55(C_5), 131.60(C_6), 129.32(C_{7+8}), 128.69(C_9), 128.53(C_{10}), 128.05(C_{11}), 127.65(C_{12+13}), 127.05(C_{14}), 126.50(C_{15}), 125.31(C_{16}), 123.93(C_{17}), 121.73(C_{18}). MS (EI, m/z (%)): 306.1[M^+, 31].

4-nitro-N-([4-nitrophenyl] carbamothioyl) benzamide (L3)

The same technique as in L1 was followed, except instead of benzoyl chloride, 10 mmol of 1.855 g of 4-nitro benzoyl chloride was employed. The product was a bright yellow. Yield: 64.98 %, mp: 196–198 °C. IR spectrum, ν, cm^{-1}: 3381 (N–H), 3045 (Ar–CH), 1678 (C=O), 1602 (C=C), 1512 and 1323 (NO_2), 1139 (C=S). ^1H NMR spectrum, δ, ppm: 8.06 d (2H, Ar–Hf+ Hf '), 8.13 d (2H, Ar–He+He'), 8.30 d (2H, Ar–Hd+Hd'), 8.42 d (2H, Ar–Hc+Hc'), 9.20 s (1H, NHa), 12.84 s (1H, NHb).MS (EI, m/z (%)): 346 [M^+, 4.5].

4-nitro-N-(p-tolylcarbamothioyl) benzamide (L4)

A similar procedure was used as in L1, but instead of benzoyl chloride, 1.855 g of 4-nitro benzoyl chloride (10 mmol) was used, and instead of 3-nitro aniline, 1.07 g of 4-methyl aniline (10 mmol) was employed. The product was a light brown color. Yield: 63.87%, mp: 136–138 °C. IR spectrum, ν, cm^{-1}: 3203 (N–H), 3039 (Ar–CH), 1687 (C=O), 1600 (C=C), 1527 and 1348 (NO2), 1157 (C=S). ^1H NMR spectrum, δ, ppm: 2.38 s (3H, CH3), 7.25 d (2H, Ar–Hf+Hf'), 7.53 d (2H, Ar–He+He'), 8.09 d (2H, Ar–Hc+Hc'), 8.37 d (2H, Ar–Hd+Hd'), 9.22 s (1H, NHa), 12.27 s (1H, NHb). ^{13}C NMR spectrum, δ_C, ppm: 177.84(C_1), 165.14(C_2), 150.66(C_3), 137.35(C_5), 137.17(C_4), 134.70(C_6), 129.65(C_{7+8}), 128.96(C_{9+10}), 124.32(C_{11+12}), 124.19(C_{13+14}), 21.19(C_{15}). MS (EI, m/z (%)): 315 [M^+, 15.44].

N-([4-chlorophenyl] carbamothioyl)-4-nitrobenzamide (L5)

The same steps as in L1 were followed, but instead of benzoyl chloride, 1.855 g of 4-nitro benzoyl chloride (10 mmol) was used, and instead of 3-nitro aniline, 1.27 g of 4-chloro aniline (10 mmol) was employed. The product was a bright yellow. Yield: 35.43 %, mp: 175–177 °C IR spectrum, ν, cm^{-1}: 3269 (N–H), 3062 (Ar–CH), 1683 (C=O), 1589 (C=C), 1533 and 1350 (NO_2), 1149 (C=S). ^1H NMR spectrum, δ, ppm: 7.42 d (2H, Ar–He+He'), 7.66 d (2H, Ar–Hf+Hf'), 8.11 d (2H, Ar–Hc+Hc'), 8.39 d (2H, Ar–Hd+Hd'), 9.24 s (1H, NHa), 12.40 s (1H, NHb). ^{13}C NMR spectrum, δ_C, ppm: 177.87(C_1), 165.08(C_2), 150.79(C_3), 136.98(C_5), 135.80(C_6), 132.58(C_4), 129.20(C_{7+8}), 128.91(C_{9+10}), 125.41(C_{11+12}), 124.42(C_{13+14}). MS (EI, m/z (%)): 335 [M^+, 13.8].

Synthesis of complexes

Cu(II) complexes were prepared with a molar ratio of 1:2. A mixture of 0.095 g of $CuCl_2.2H_2O$ (0.5 mmol) and 1 mmol of L1, L2, L3, L4, or L5 was dissolved in 10:10 mL of MeOH + acetone. Each reaction separately was heated in a water bath with stirring and refluxing for 2 hours. Finally, the precipitated products were cooled, filtered, and washed several times with distilled water, ethanol, and diethyl ether. After drying, the following were obtained:

$[Cu(L1)_2Cl_2]\cdot 2H_2O$ (1): Yellow color. Yield: 63 %, mp: 200 °C. IR spectrum, ν, cm^{-1}: 3151 (O– H), 3197 (N–H), 3037 (Ar–CH), 1678 (C=O), 1598 (C=C), 1527 and 1348 (NO_2), 1163 (C=S). μeff (B.M): 1.061. Molar conductivity (DMSO, $Ohm^{-1}cm^2mol^{-1}$): 28.4. MS (ESI): 772 [M^+].

$[Cu(L2)_2Cl_2]\cdot 2H_2O$ (2): Yellow color. Yield: 56 %, mp: >208.7 °C. IR spectrum, ν, cm^{-1}: 3053 (O-H), 3143 (N–H), 3001 (Ar–CH), 1668 (C=O), 1629 (C=C), 1527 and 1330 (NO_2), 1153 (C=S). μeff (B.M): 1.12. Molar conductivity (DMSO, $Ohm^{-1}cm^2mol^{-1}$): 32.9. MS (ESI): 782 [M^+].

$[Cu(L3)_2Cl_2]$ (3): Dark yellow color. Yield: 70 %, mp: >224 °C. IR spectrum, ν, cm^{-1}: 3051 (O–H), 3115 (N–H), 3001 (Ar–CH), 1689 (C=O), 1604 (C=C), 1516 and 1330 (NO_2), 1166 (C=S). μeff (B.M): 1.06. Molar conductivity (DMSO, $Ohm^{-1}cm^2mol^{-1}$): 32.7. MS (ESI): 828 [M^+].

$[Cu(L4)_2Cl_2]\cdot 2H_2O$ (4): Orange color. Yield: 68 %, mp: 228 °C. IR spectrum, ν, cm^{-1}: 3153 (O–H), 3113 (N–H), 3039 (Ar–CH), 1683 (C=O), 1598 (C=C), 1529 and 1344 (NO_2), 1157 (C=S). μeff (B.M): 1.087. Molar conductivity (DMSO, $Ohm^{-1}cm^2mol^{-1}$): 34.7. MS (ESI): 801 [M^+].

$[Cu(L5)_2Cl_2]\cdot 4H_2O$ (5): Light orange color. Yield: 38 %, mp: 209 °C. IR spectrum, ν, cm^{-1}: 3159 (N–H), 3041 (Ar–CH), 1681 (C=O), 1598 (C=C), 1531 and 1346 (NO_2), 1159 (C=S). μeff (B.M): 1.077. Molar conductivity (DMSO, $Ohm^{-1}cm^2mol^{-1}$): 21.3. MS (ESI): 878 [M^+].

Evaluation of anti-cancer activity

The MTT (3-[4,5-dimethylthiazol-2-yl]-2,5-diphenyltetrazolium bromide) assay,[17,18] was employed to test the *in vitro* cytotoxicity of the test compounds. The human breast cancer cell line (MCF7) was purchased from the National Cell Bank of Iran (Institute Pasteur, Iran).

Cells were grown in RPMI-1640 (Gibco) and DMEM medium (Gibco), respectively, with 10% FBS (Gibco) supplemented with antibiotics (100 U/ml penicillin and 100 µg/ml streptomycin). The cells were maintained at 37°C in humidified air containing 5% CO_2 and passed with trypsin/EDTA (Gibco) and phosphate-buffered saline (PBS) solutions. The culture media and conditions used to grow cells as 3D colonies were the same as for monolayer cell cultures.

Molecular docking

The molecular docking study of test compounds 1 and 2 (1) and (2) was conducted using MOE (2019).[19] The protein crystal structure of the used receptors, 4OAR and 5KCV, was acquired from the Protein Data Bank (PDB) (https://www.rcsb.org/ structure). The processing of test compounds, proteins, and docking procedures was carried out following the literature.[20,21]

Results and Discussion

Production of the ligands

The reaction between ammonium thiocyanate and some benzoyl chloride derivatives at a 1:1 mole ratio produced benzoyl isothiocyanate derivatives, as shown in Scheme 1(ia), while the reaction between the product from the first step and some amine derivatives at a 1:1 mole ratio resulted in thiourea benzamide derivative ligands L1, L2, L3, L4, and L5, as presented in Scheme 1(ib). The reaction of these ligands with Cu(II) ions in methanol and acetone produced the complexes (1-5) in a 1:2 ratio (metal: ligand) as highlighted in Scheme 1(ii).

Characteristics of the ligands

Mass spectrometry, infrared, and nuclear magnetic resonance techniques were used to identify the correct structure of ligands. EI-MS spectra of prepared ligands were given molecular ion peaks at m/z= 301.1, 306.1, 346, 315, and 335 for L1, L2, L3, L4, and L5, respectively with varying relative abundance, which corresponds to the molecular weight of the compounds having the molecular formula $(C_{14}H_{11}N_3O_3S_1)^+$, $(C_{18}H_{14}N_2O_1S_1)^+$, $(C_{14}H_{10}N_4O_5S_1)^+$, $(C_{15}H_{13}N_3O_3S_1)^+$, $(C_{14}H_{10}ClN_3O_3S_1)^+$, and appearance of a set of fragments that show the proposed compound was present. ^{1}HNMR spectra of ligands (Figure 1) showed singlet, doublet, and multiplet signals at the range of 7.25–8.80 ppm which can be attributed to aromatic protons.[22] The appearance of a singlet signal in the spectra confirmed the presence of the amide group (-NH) at 9.20, 9.28, 9.20, 9.22, and 9.24 ppm for L1, L2, L3, L4, and L5 respectively, while the (-NH) group's proton signal showed up as a singlet at 12.90, 12.76, 12.84, 12.27, and 12.40 ppm.[23] The spectra of ligand L4 showed a singlet signal at 2.38 due to (-CH_3) protons.

As observed in Figure 2, ^{13}CNMR spectra of ligands demonstrate the correct skeletal structure of the prepared ligands. The signals in the 180.09–177.84 ppm range correspond to carbons in the C=S group, whereas the 167.24–165.08 ppm range corresponds to carbon in the carbonyl group.[11] The signals with the range 121.73-150.79 ppm are attributed to the aromatic carbons, and the signal at 21.19 ppm in L4 spectra is attributed to the aliphatic carbons (CH_3).[22] The infrared spectra for prepared compounds showed medium and strong intensity bands at a range of 3442–3107 cm^{-1} assigned to the (N-H) group's stretching vibration. This indicates the formation of ligands, and one or two bands at the range between 3097–3016 cm^{-1} were observed due to symmetrical and asymmetrical stretching vibration of (C-H) aromatic for both ligands and complexes. Furthermore, the strong band at range 1687–1668 cm^{-1} is attributed to the stretching vibration of the carbonyl group, which shifts in complex compounds as a result of coordination between metals and ligands. The stretching vibration of the (C=C) group of the aromatic structure is indicated by a medium intensity band at 1629-1589 cm^{-1} regions. Additionally, the compounds were characterized by the appearance of a medium band at 1159 –1139 cm^{-1}, which is associated with the (C=S) group. This band shifts and loses intensity in coordination complexes as proof of the involvement of the C=S group in the coordinate process. The spectra of complexes were also characterized by the emergence of bands in the fingerprint area due to the coordination between metals and ligands. These two strong bands at the ranges (1533-1512 cm^{-1}) and (1350-1323 cm^{-1}) are attributable to the stretching vibration of the NO_2 group.

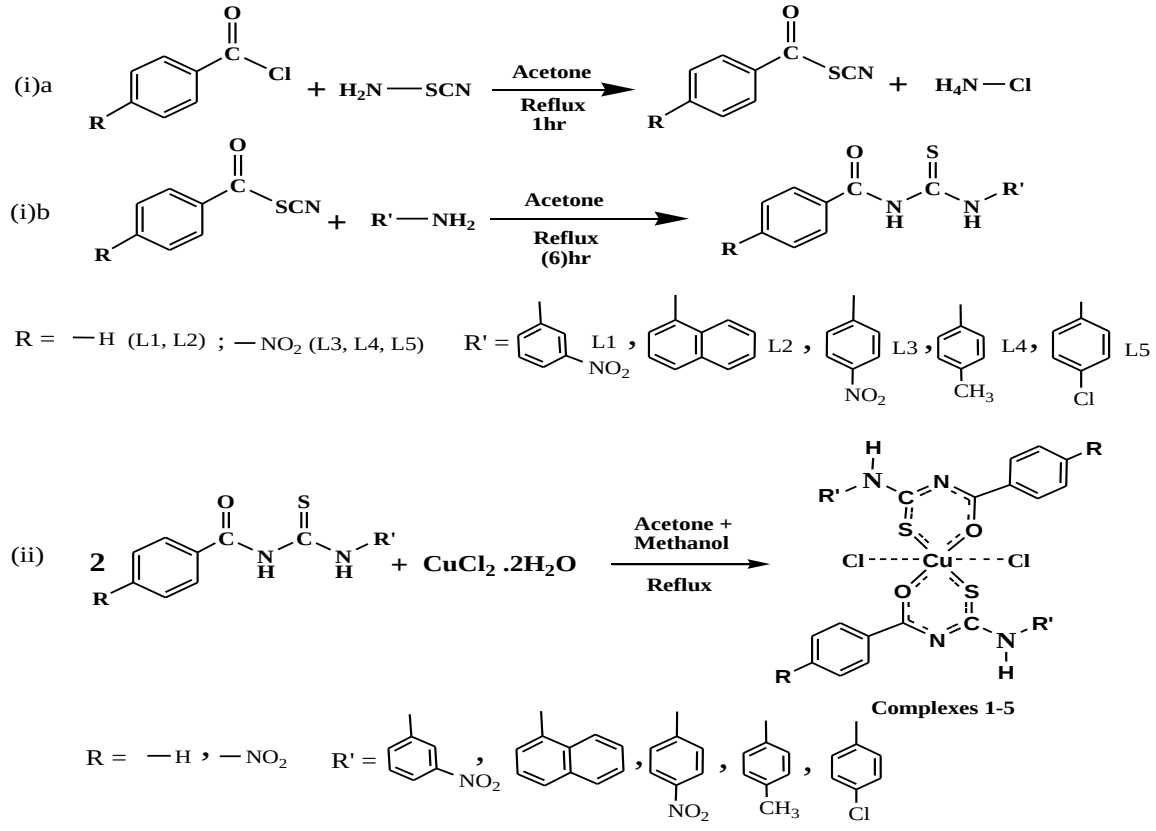

Scheme 1: Preparation pathway to ligands and metal complexes

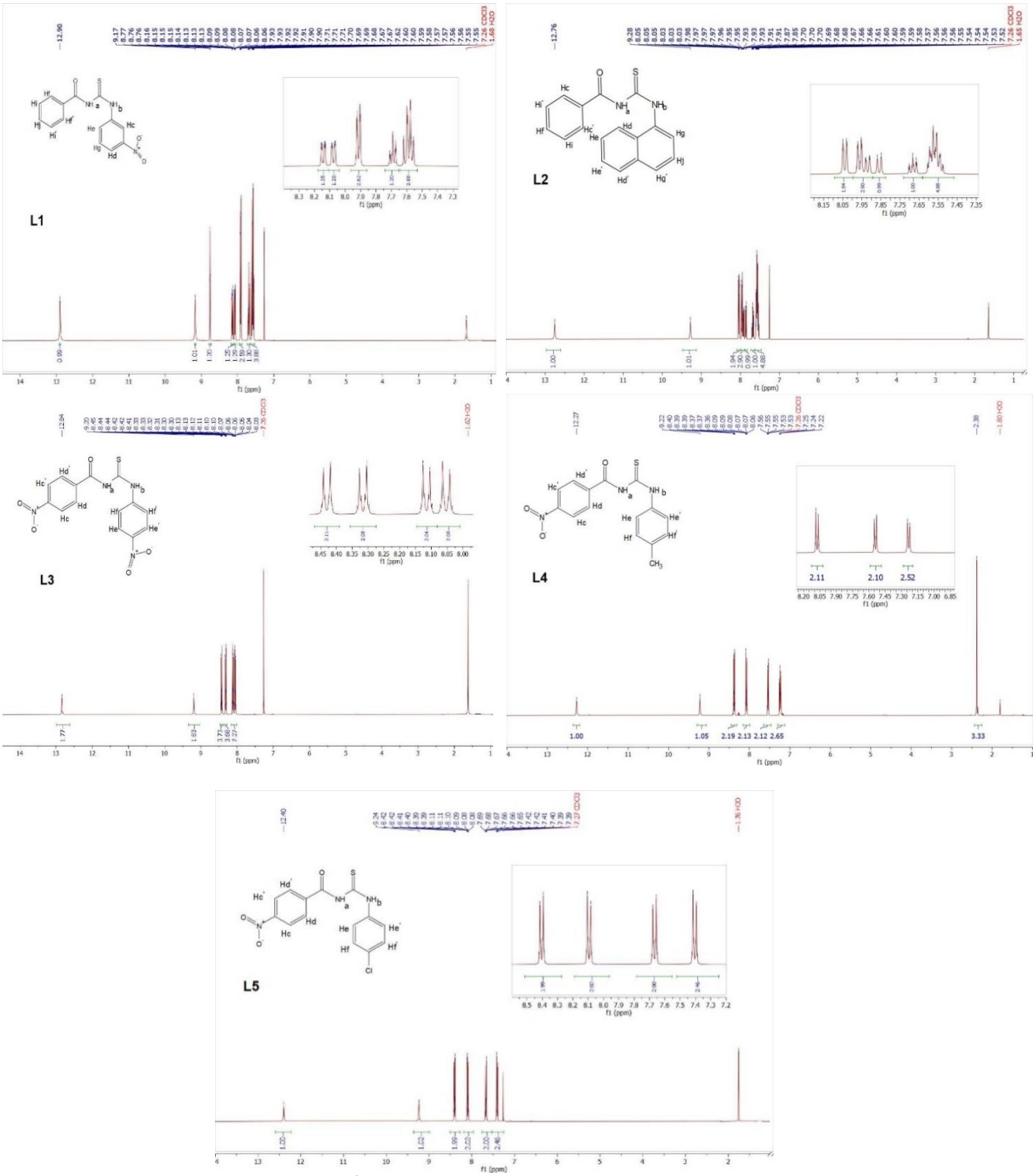

Figure 1: ^{1}H-NMR spectra of ligands L1, L2, L3, L4, and L5.

Characteristics of the metal complexes

ESI-MS spectra of complexes showed molecular ion peaks at m/z= 772, 782, 828, 801, and 878, which correspond to the molecular formula of the complexes (1)-(5). The presence of these compounds was confirmed by fragments in the complexes. The molar conductivity values of complexes were within the range (18.3–32.9 $Ohm^{-1}cm^{2}mol^{-1}$), indicating that no counter ions with non-electrolyte characteristics were present.[25] The values of the effective magnetic moment (μ_{eff}) of the copper complexes (1), (2), (3), (4), and (5) were 1.06, 1.12, 1.06, 1.08, and 1.07 B.M., respectively. These results indicate that the complexes showed paramagnetic properties because there is one electron that is not paired with an electron configuration $[Ar]3d^{9}4s^{0}4p^{0}$. The reason for the low magnetic moment values may be due to the anti-ferromagnetic effect.[26] Therefore, the expected geometry of copper complexes is octahedral and hybridization is $sp^{3}d^{2}$.[27,28] Figure 3 and Table 1 show the stages of thermal decomposition of metal complexes. The decomposition stages and thermograms refer to the presence of crystallization water, in addition to the two chlorine atoms in the structure of complex molecules. This decomposition occurs in the early stages of disintegration with a range between 50-272°C,[29] while the other stages include the loss of some of the ligands.

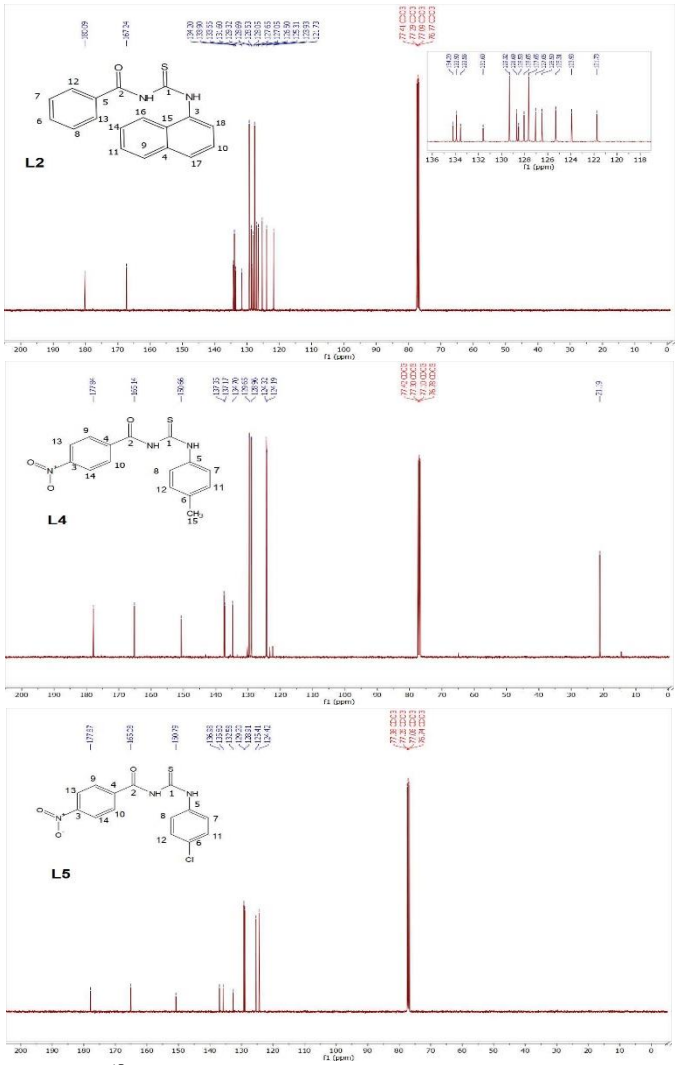

Figure 2: ^{13}C-NMR spectra of ligands L2, L4, and L5.

Characteristics of the ligands based on scanning electron microscopy (SEM) and energy dispersive X-ray spectroscopy (EDX)

Scanning electron microscopy (SEM) is a surface imaging method that is quite capable of imaging the particle sizes, distribution, shapes, and morphology of different micromaterials, as well as giving information about the shape of the particles, the nature of agglomeration between them, and the nature of smooth or porous surfaces.[30] The principle of the scanning electron microscope depends on the interaction between the electron beam emitted by the instrument and the sample material, and it can be used to describe microelements based on X-rays. The EDX analysis requires producing X-rays in the sample scanning area.[31] A scanning electron microscope was employed in this study to analyze the composition of the samples. Figure 4a shows an SEM image demonstrating the formation of the L5 ligand in a semi-spherical shape, indicating the presence of clusters in the prepared ligand. Also, the presence of many voids or gaps on its surface that increase the surface area of the prepared ligand was observed. The particles of the complex are displayed in Figure 4b. Due to the strong attraction forces and the widening of the spaces between them, the texture of its outer surface changed, taking on the shape of clusters.[32] The size of the particles was 73.69 nm for the ligand and 98.25 nm for the complex, suggesting that they are nanoparticles.[33]

The elemental analysis and the percentage composition of the ligand and complex were determined by EDX analysis. The number of X-rays that were detected and processed by the detector is indicated on the y-axis, and the energy level of these elements is shown on the x-axis. The results (Figure 5a) clearly indicate that the elements in ligand L5 have a weight ratio of C = 58.8, Cl= 16.7, S = 15.7, and O = 8.8, while the elements in complex 5 have a weight ratio of C = 52.9, Cl = 11.9, S = 11.5, Cu = 10.0, N = 8.0, and O = 5.7. This observation confirms the presence of the elements constituting the ligand and complex only, and there are no impurities in the samples. In addition to the appearance of a peak of the gold element, which is due to the base of the device on which the sample was deposited.[32]

Anticancer properties of the ligands and complexes

The toxicity of synthesized compounds against breast cancer cell lines (MCF-7) was studied using five different concentrations per compound. The inhibition activity of compounds was calculated at each concentration, in addition to the concentration values of the maximum half-effect IC_{50}.

Table 1: Thermogravimetric characteristics of the complexes produced from thiourea benzamide derivatives

Complex /M.Wt.	Stage	Temp. range (℃)	Decomposition part	Weight loss %	
				Observed	Calculated
$[Cu(L1)_2Cl_2].2H_2O$ 773 g/mol	1	25-216	$2H_2O$ +2Cl	11.42	13.84
	2	216-270	$2(C_7H_6NO)$	36.17	36.07
	3	270-805.5	$C_6H_5N_2O_2$	34.92	32.19
$[Cu(L2)_2Cl_2].2H_2O$ 783 g/mol	1	25-259.5	$2(C_{10}H_7)$ + $2H_2O$ +2Cl	45.97	46.14
	2	259.5-804	$2(C_6H_5)$	34.17	36.57
$[Cu(L3)_2Cl_2]$ 827 g/mol	1	25-298	$2(C_6H_4NO_2)$ + 2Cl	37.01	38.09
	2	298-802	$C_6H_4NO_2$ + NH	25.53	25.32
$[Cu(L4)_2Cl_2].2H_2O$ 801 g/mol	1	25-246.6	$2H_2O$ + 2Cl + $2(NO_2)$	23.18	24.84
	2	246.6-596.6	$2(C_8H_8NS)$	49.57	49.83
	3	596.6-805.6	NH	4.03	4.96
$[Cu(L5)_2Cl_2].4H_2O$ 878 g/mol	1	25-217.5	$4H_2O$	10.24	8.20
	2	217.5-240.8	4Cl	17.52	17.61
	3	240.8-363	C_7H_5NS	41.62	40.66
	4	363-805.5	NO_2	12.11	11.67

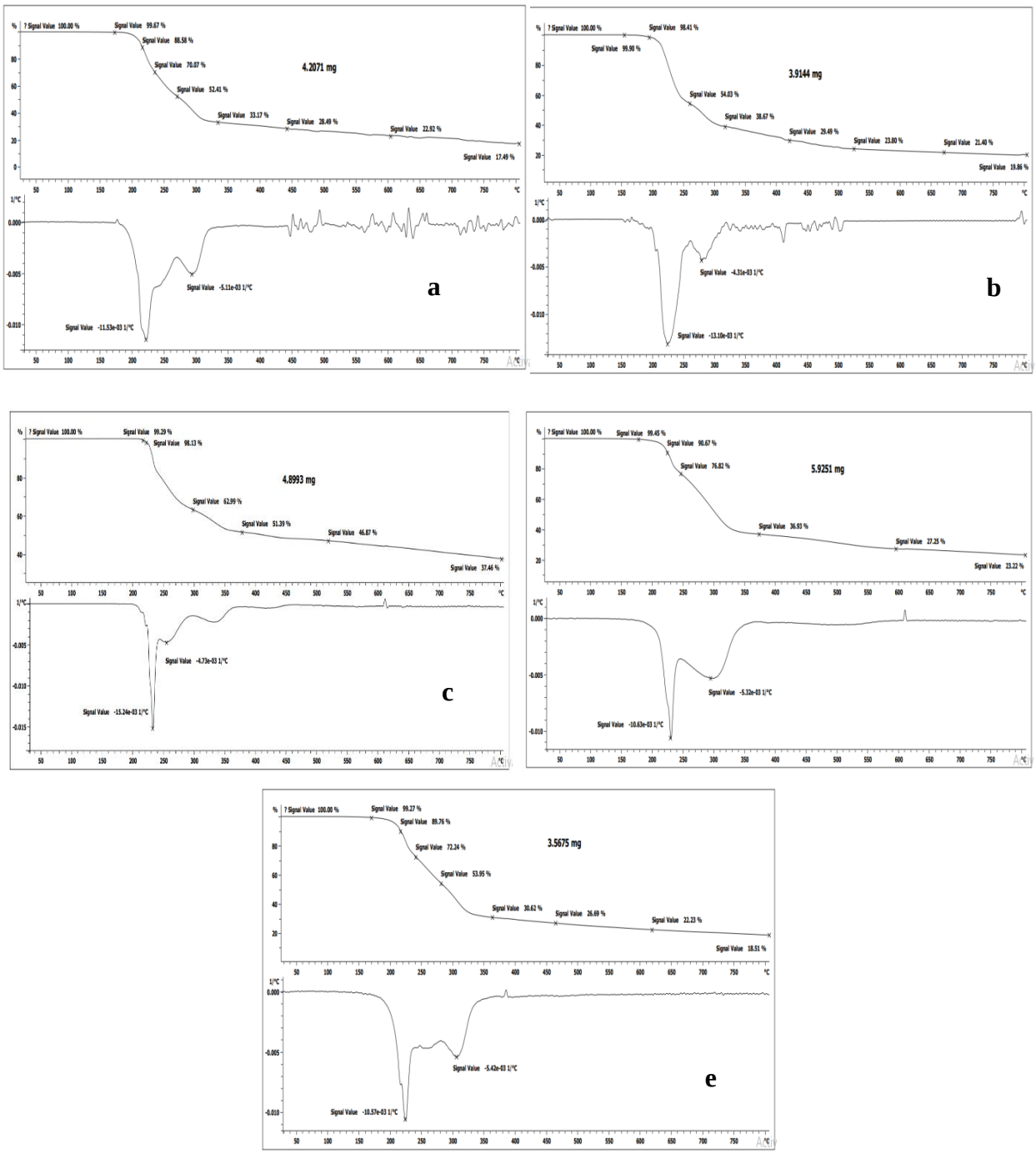

Figure 3: Thermo-gravimetric patterns of complexes $[Cu(L1)_2Cl_2].2H_2O$(a),$[Cu(L2)_2Cl_2].2H_2O$(b), $[Cu(L3)_2Cl_2]$(c), $[Cu(L4)_2Cl_2]\cdot 2H_2O$(d), $[Cu(L5)_2Cl_2]\cdot 4H_2O$(e).

The prepared ligands showed varying efficacy in killing cancer cells, as evident by the values of IC_{50} (Table 2). As for the prepared complexes, they demonstrated high effectiveness through their low IC_{50} values (IC_{50}=4.03 and 4.66 µg/mL) when compared to the effectiveness of ligands that were prepared from them.[34,35] This explains the high effectiveness of copper complexes and their capacity to penetrate the cell membrane of cancer cells, which has been proven in numerous studies.

Molecular docking findings

The study of the molecular docking of complexes (1) and (2) was conducted against breast cancer proteins, MCF-7 cell line, which are ERα (PDP: 3ERT), PR (PDP: 4OAR), EGFR (PDP: 2J6M), mTOR (PDP: 4DRH), CDK2 (PDP: 4FX3), CDK6 (PDP: 3NUP), and Akt (PDP: 5KCV).[36-39] There was the strongest interaction with 4OAR and 5KCV proteins, where it gave the highest affinity energy (S) and the lowest RMSD value of 23, as presented in Table 3. Docking analysis is used to determine how amino acid residues and hydrogen bonds of target proteins interact with complexes (1) and (2).[40] Figure 6 shows the 2D and 3D forms of interactions. It is evident from the figure that there are five hydrogen bonds between complex (1) and the 4OAR protein, four of which are donor bonds through the S, N, and Cl atoms, and one acceptor bond with the oxygen atom. Meanwhile, complex (2) interacted with protein 4OAR by forming a donor hydrogen bond with the amino acid Cys-891 by a nitrogen atom, in addition to, forming a two pi-interaction of the hydrophobic phenyl moiety with the amino acids Phen-895 and Phen-794. On the other hand, it was observed that complex (1) binds to protein 5KCV by forming two donor hydrogen

bonds, one with the amino acid Asp-292 through the sulfur atom and the other with Thr-82 through the nitrogen atom, in addition to the formation of three pi-interactions with the amino acids Gly-294, Trp-80, and Gln-79.

The interaction of complex (2) with protein 5KCV involved the formation of three hydrogen bonds, two of which were donor and one acceptor, all of which involved sulfur atoms and the amino acids Lle-84, Asp-292, and Gly-276, as well as a two pi-interaction of the hydrophobic phenyl moiety with the amino acids Lys-276 and Asn-279.

Conclusion

The characterization techniques used confirmed the validity of the proposed structures of the synthesized compounds. The stoichiometry of metal: ligand in the complexes confirms that the analytical data ratio is 1:2. In the sulfur atom of the (C=S) group and the oxygen atom of the carboxyl group, the ligands L1, L2, L3, L4, and L5 functioned as a bidentate ligand type S_1O_1 with Cu(II). In addition, the geometry of complexes was octahedral (sp^3d^2) with Cu(II). The complexes have non-electrolyte properties and contain lattice water molecules. SEM study demonstrated the changes in surface morphology between ligand L5 and complex 5, which are approximately on the nanoscale. EDX analysis demonstrated the presence of the two compounds' constituent parts. The biological activity study demonstrated that the copper complexes (1) and (2) are superior to the ligands employed to produce the complexes in their ability to effectively inhibit breast cancer (MCF-7) cell line. The molecular docking study indicated that compounds (1) and (2) target PR and Akt proteins belonging to line breast cancer cells (MCF-7). The findings of this study suggest that copper complexes with thiourea benzamide compounds have biological activities against cancer cells (MCF-7). It is therefore recommended that the preparation of several thiourea benzamide derivatives could be used in research on various cancer cells or other types of breast cancer cell lines as well as for therapeutic purposes (drug).

Conflict of Interest

The authors declare no conflict of interest.

Authors' Declaration

The authors hereby declare that the work presented in this article is original and that any liability for claims relating to the content of this article will be borne by them.

Acknowledgements

The authors extend their appreciation to the Department of Chemistry, Faculty of Education for Pure Sciences, University of Basrah for providing all necessary research facilities, including the laboratory.

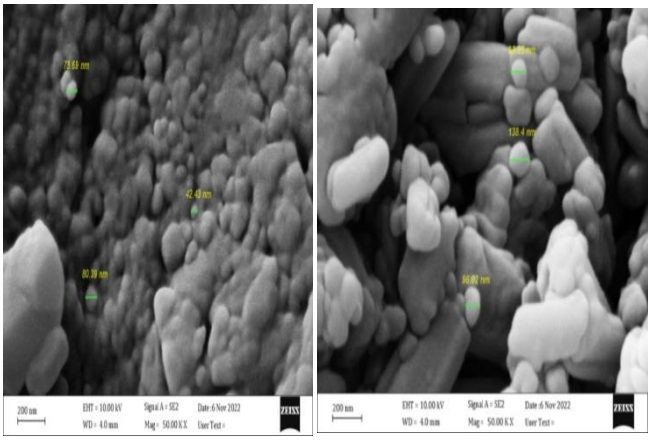

Figure 4: Scanning electron microscopy images. a: L5 ligand particles; b: Complex $[Cu(L5)_2Cl_2]\cdot 4H_2O$ particles.

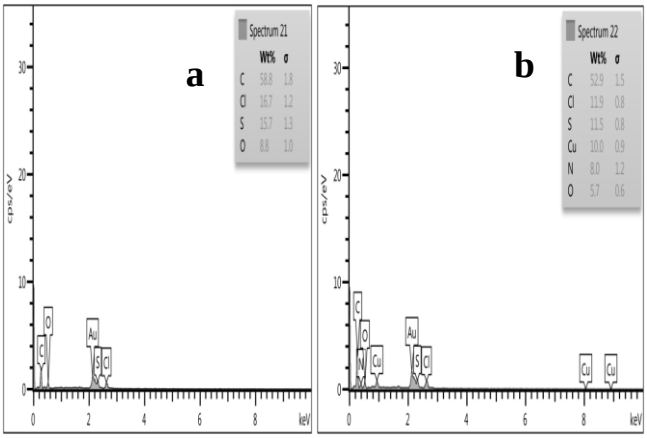

Figure 5: Energy-dispersive X-ray spectroscopy (EDX) spectra. a: Ligand L5; b: Complex$[Cu(L5)_2Cl_2]\cdot 4H_2O$.

Table 2: Inhibition ratio of MCF-7 cell line and IC_{50} values of the test compounds

Ligand	Concentration (µg/mL)					IC_{50} (µg /mL)
	6.25	12.5	25	50	100	
	Cell inhibition (%)					
L1	88.05	81.84	66.67	63.22	46.32	92.09
L2	97.47	73.68	60.34	56.55	46.09	66.07
L3	87.70	73.79	69.77	66.09	56.09	188.94
L4	94.14	90.34	81.49	64.83	62.76	237.87
L5	95.52	84.60	72.64	68.97	56.55	167.09
Complex	**Concentration (µg/mL)**					**IC_{50} (µg/mL)**
	0.781	**1.562**	**3.125**	**6.25**	**12.5**	
	Cell inhibition (%)					
$[Cu(L1)_2Cl_2].2H_2O$	97.96	86.33	76.98	15.59	16.19	4.03
$[Cu(L2)_2Cl_2].2H_2O$	112.95	102.76	85.61	38.25	18.35	4.66

ISSN 2616-0684 (Print)
ISSN 2616-0692 (Electronic)

Table 3: Molecular docking of compounds (1) and (2) with target 4OAR and 5KCV proteins

Proteins (Receptors)	Complex	RMSD*	Affinity energy (S) Kcal/mol	Interaction		
				Type	Amino acid	H-Bonding distance(Å)
4OAR	(1)	1.831	-8.626	H-Bonding	Cys891	3.39
				H-Bonding	Cys891	3.22
				H-Bonding	Met759	3.28
				H-Bonding	Gln725	2.20
				H-Bonding	Asn719	3.15
				H-Bonding	Cys891	2.73
	(2)	1.483	-8.828	H- *pi* –Bonding	Phen895	-
				H- *pi* –Bonding	Phen794	-
				H-Bonding	Asp292	3.76
				H-Bonding	Thr82	2.66
5KCV	(1)	1.919	-9.300	H- *pi* –Bonding	Gly294	-
				H- *pi* –Bonding	Trp80	-
				H- *pi* –Bonding	Gln79	-
				H-Bonding	Lle84	3.93
				H-Bonding	Asp292	3.24
	(2)	1.941	-9.564	H-Bonding	Gly294	3.09
				H- *pi* –Bonding	Lys276	-
				H- *pi* –Bonding	Asn279	-

*: Root mean square deviation

(a)

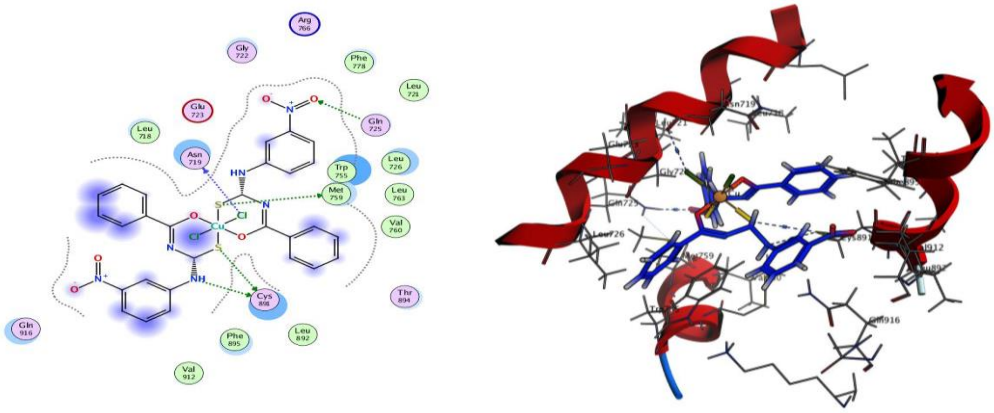

(b)

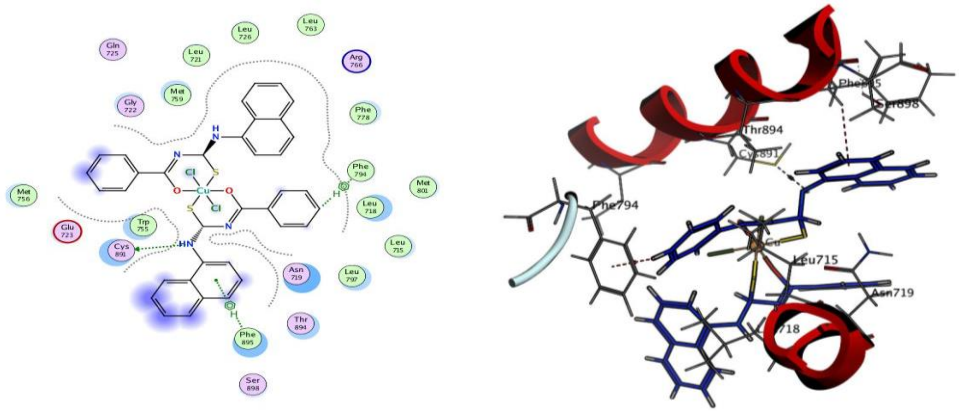

(c)

(d)

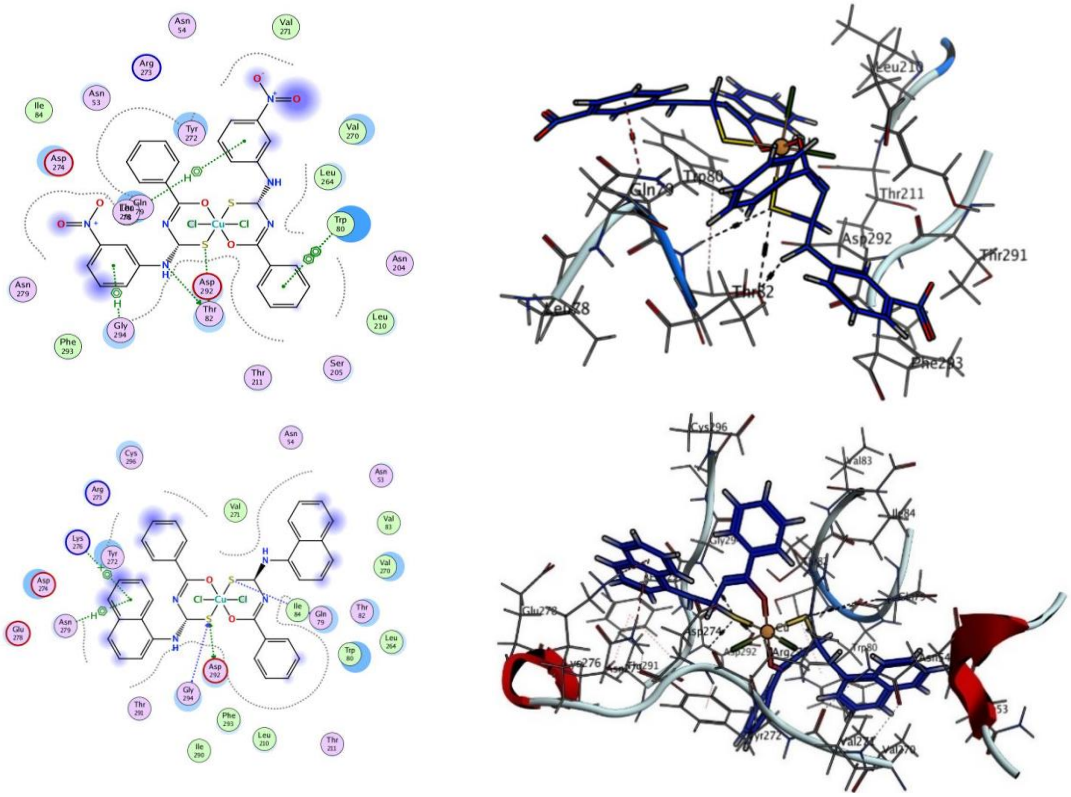

Figure 6: 2D and 3D forms. a: Complex 1 with target proteins 4OAR; b: Complex 2 with target proteins 4OAR; c: Complex 1 with target proteins 5CVK; d: Complex 2 with target proteins 5CVK.

References

1. Ili M, Bucos M, Dumitracu F, Cırcu V. Mesomorphic behavior of N-benzoyl-N′-aryl thioureas liquid crystalline compounds. J Mol Str. 2011; 987: 1–6. Doi:10.1016/j.molstruc.2010.11.037
2. Singh G, Saroa A, Rani S, Girdhar S, Sahoo S, Choquesillo-Lazarte D. Substituted phenyl urea and thiourea silatranes: Synthesis, characterization, and anion recognition properties by photophysical and theoretical studies. Polyhedron. 2016; 112: 51-60. Doi:10.1016/j.poly.2016.03.036
3. Saeed A, Ashraf S, White JM, Soria DB, Franca CA, Erben MF. Synthesis, X-ray crystal structure, thermal behavior, and spectroscopic analysis of 1-(1-naphthoyl)-3-(halo-phenyl)-thioureas complemented with quantum chemical calculations, Spectrochimica Acta. 2015; 150: 409-418. Doi:10.1016/j.saa.2015.05.068
4. Halim AN, Ngaini Z. Synthesis and characterization of halogenated bis(acylthiourea) derivatives and their antibacterial activities. Phosphorus, Sulfur, and Silicon and the Related Elements. 2017; 192(9): 1012–1017. Doi:10.1080/10426507.2017.1315421
5. Arslan H, Duran N, Borekci G, Ozer CK, Akbay C. antimicrobial activity of some thiourea derivatives and their nickel and copper complexes. Molec. 2009; 14: 519-527. Doi:10.3390/molecules14010519
6. Al-Merhj SA. Synthesis and characterization of new thiourea complexes. J Fac Basic Edu. 2012; 73: 45-53.
7. Ozer CK, Arslan H, VanDerveer D, Binzet G. Synthesis and characterization of N-(alky(aryl) carbamothioyl)cyclohexanecarboxamide derivatives and their Ni(II) and Cu(II) complexes. J Coord Chem. 2009; 62: 266-276. Doi:10.1080/00958970802209623
8. Stefanska J, Szulczyk D, Koziol AE, Miroslaw B, Kedzierska E, Fidecka S, Busonera B, Sanna G, Giliberti G, La Colla P, Struga M. Disubstituted thiourea derivatives and their activity on CNS: Synthesis and biological evaluation. Eur J Med Chem. 2012; 55: 205-13. Doi:10.1016/j.ejmech.2012.07.020
9. Shakeel A, Altaf AA, Qureshi AM, Badshah A. Thiourea derivatives in drug design and medicinal chemistry: a short review. J Drug Des Med Chem. 2016; 2(1): 10–20. Doi: 10.11648/j.jddmc.20160201.12
10. Alkherraz AM, Lusta IZ, Zubi EA. Synthesis and use of thiourea derivative (1-phenyl-3-benzoyl-2-thiourea) for extraction of cadmium ion. Inter Scho Scien Res Innov. 2014; 8(2): 116–118.
11. Silveira RG, Catão AJ, Cunha BN, Almeida F, Correa RS, Diniz LF, Tenório JC, Ellena J, Kuznetsov AE, Batista AA. Facile synthesis and characterization of symmetric N-[(phenylcarbonyl) carbamothioyl] benzamide thiourea: Experimental and theoretical investigations. J Braz Chem Soc. 2018; 29(12): 2502-2513. Doi:10.21577/0103-5053.20180129
12. Yamin BM, Yusof MSM, Jusoh RH. 2-Methyl-N-[(3-methyl-2-pyridyl carbamothioylbenzamide. Acta Cryst. E64, 2008; o833. Doi:10.1107/S1600536808009513
13. Al-Jibori SA, Dayaaf NA, Mohammed MY, Merzweiler K, Wagner Ch, Hogarth G, Richmond MG. cis–trans Isomerism at Square-Planar MN2S2 Centers (M = Pd, Pt): Crystal Structures of N-Phenyl-N-(2-thiazoyl)thiourea Complexes trans-Pd(S2N3C10H8)2 and cis-Pt(S2N3C10H8)2 and

Density Functional Calculations. J Chem Crystallogr. 2013; 43: 365–372.Doi:10.1007/s10870-013-0429-7
14. Pandey SK, Pratap S, Rai SK, Marverti G, Kaur M, Jasinsk JP. Synthesis, characterization, Hirshfeld surface, cytotoxicity, DNA damage and cell cycle arrest studies of N, N-diphenyl-N'-(biphenyl-4-carbonyl/4-chlorobenzoyl) thiocarbamides. J. Mol Struc. 2019; 1186: 333-344. Doi:10.1016/j.molstruc.2019.03.057
15. Abdel–Hadi KA, Abdel-Razik A, Shoukry MM, Shoheib ShM. Egypt J Chem.1996; 39 (2), 179.
16. Saeed A, Qamar R, Fattah TA, Flörke U, Erben MF. Recent developments in chemistry, coordination, structure and biological aspects of 1-(acyl/aroyl)-3-(substituted) thioureas. Res Chem Interm. 2017; 43: 3053-3093. Doi:OI 10.1007/s11164-016-2811-5.
17. Al-Asadi RH, Al-Masoudi WA, Abdu Al-Rassol KS. Synthesis, biological activity, and computational study of some new unsymmetrical organotellurium compounds derived from (2-amino-5-carboxyphenyl) mercury(II) chloride. Asian J Chem. 2016; 28(6): 1171-1176. Doi:10.14233/ajchem.2016.19139.
18. Rollando R, Monica E, Aftoni MH, In vitro cytotoxic potential of sterculia quadrifida leaf extract against human breast cancer cell lines. Trop J Nat Prod Res. 2022; 6(8):1228-1232 Doi:10.26538/tjnpr/v6i8.12
19. Scholz C, Knorr S, Hamacher K, Schmidt B. DOCKTITE—A highly versatile step-by-step workflow for covalent docking and virtual screening in the molecular operating environment. J Chem Inf Model. 2015; 55(2): 398–406. Doi:10.1021/ci500681r
20. Mutlaq DZ, Al-Shawi AA, Al-Asadi RH. Synthesis, characterization, anticancer activity, and molecular docking of novel maleimide–succinimide derivatives. Egypt Pharm J. 2021. Doi: 10.4103/epj.epj_26_21
21. Elkanzi NA, Ali MA, Albqmi M , Abdou A. New benzimidazole-based Fe (III) and Cr (III) complexes: Characterization, bioactivity screening, and theoretical implementations using DFT and molecular docking analysis. Appl Organomet Chem. 2022; 36(11): e6868. Doi:10.1002/aoc.6868
22. Faye F, Sylla-Gueye R, Thiam IE, Orton J, Coles S, Gaye M. Synthesis, characterization and crystal structure of 1-(2-benzamidophenyl)-3-benzoylthiourea hemihydrate. Sci J Chem. 2020; 8(6): 131-135. Doi:10.11648/j.sjc.20200806.11
23. Saad FA. Co-ordination chemistry of some first-row transition metal complexes with multi-dentate ligand (1-benzoyl-3-(4-methylpyridin-2-yl) thiourea), spectral, electrochemical and X – ray single crystal studies. Int J Electrochem Sci. 2014; 9: 4761 – 4775.
24. Abd Halim AN, Ngaini Z. Synthesis and bacteriostatic activities of bis (thiourea) derivatives with variable chain length. J Chem. 2016; 2739832: 7. Doi:10.1155/2016/2739832
25. Nawar FA, AL-Asadi RH, Abid DS. Synthesis, antibacterial activity and DFT calculations of some thiazolidine-4-carboxylic acid derivatives and their complexes with Cu(II), Fe(II) and VO(II). Egypt J Chem. 2020. Doi:10.21608/ejchem.2019.16096.1986
26. Lo SMF, Chui SSY, Shek LY, Lin Z, Zhang XX, Wen GH, Williams ID. Solvothermal synthesis of a stable coordination polymer with copper-i−copper-ii dimer units: [Cu4{1,4-C6H4(COO)2}3(4,4‘-bipy)2]n. J Am Chem Soc. 2000; 122(26): 6293–6294. Doi:10.1021/ja000416c.
27. Khulbe RC, Singh RP, Bhoon YK. Copper(II), nickel(II) and cobalt(II) complexes of pyridyl and quinolylhydrazones of isatin and methylisatin: Ligand dependent stereochemistry. Trans Met Chem.1983; 8: 59-61. Doi:10.1007/BF00618802
28. Elkanzi NA , Hrichi H, Salah H, Albqmi M, Ali MA, Abdou A. Synthesis, physicochemical properties, biological, molecular docking and DFT investigation of Fe(III), Co(II), Ni(II), Cu(II) and Zn(II) complexes of the 4-[(5-oxo-4,5-dihydro-1,3-thiazol-2-yl)hydrazono]methyl}phenyl 4-methylbenzenesulfonate Schiff-base ligand. Inorg Chem Comm. 2023; 148:110331. Doi:10.1016/j.inoche.2022.110331
29. Bhattacharjee CR, Goswami P, Mondal P. Synthesis, reactivity, thermal, electrochemical and magnetic studies on iron(III) complexes of tetradentate Schiff base ligands. Inorganica Chimica Acta. 2012; 387: 86-92. Doi:10.1016/j.ica.2011.12.056
30. Gnanamoorthy P, Karthikeyan V, Prabu VA. Field emission scanning electron microscopy (FESEM) characterization of the porous silica nanoparticulate structure of marine diatoms. J Porous Mater. 2014; 21: 225-233. Doi:10.1007/s10934-013-9767-2
31. Ellingham TD, Thompson TJU, Islam M. Scanning electron microscopy–energy-dispersive X-Ray (SEM/EDX): A rapid diagnostic tool to aid the identification of burnt bone and contested cremains. J Foren Sci. 2017; 63(2): 504-510. Doi:10.1111/1556-4029.13541
32. Din SU, Iqbal H, Haq S, Ahmad P, Khandaker MU, Elansary HO, Al-Harbi FF, Abdelmohsen ShAM, Zin El-Abedin TK. Investigation of the biological applications of biosynthesized nickel oxide nanoparticles mediated by Buxus wallichiana extract. Crystals. 2022; 12(2): 146. Doi:10.3390/cryst12020146.
33. Hoshyar N, Gray S, Han H, Bao Ga. The effect of nanoparticle size on in vivo pharmacokinetics and cellular interaction, Nanomedicine (Lond). 2016; 11(6): 673–692. Doi: 10.2217/nnm.16.5.
34. Ji P, Wang P, Chen H, Xu Y, Ge J, Tian Z, Yan Z. Potential of copper and copper compounds for anticancer applications. Pharmaceut. 2023; 16(2): 234. Doi:10.3390/ph16020234
35. Molinaro C, Martoriati A, Pelinski L, Cailliau K. Copper complexes as anticancer agents targeting topoisomerases i and II. Cancers (Basel). 2020; 12(10): 2863.Doi: 10.3390/cancers12102863
36. Fagan DH, Fettig LM, Avdulov S, Beckwith H, Peterson MS, Ho YY, Wang F, Polunovsky VA, Yee D. Acquired tamoxifen resistance in MCF-7 breast cancer cells requires hyperactivation of eIF4F-mediated translation. Horm Cancer. 2017; 8(4): 219-229.Doi: 10.1007/s12672-017-0296-3
37. Venugopal K, Ahmad H, Manikandan E, Thanigai KA, Kavitha K, Moodley M, Rajagopal K, Balabhaskar K, Bhaskar M. The impact of anticancer activity upon Beta vulgaris extract mediated biosynthesized silver nanoparticles (ag-NPs) against human breast (MCF-7), lung (A549) and pharynx (Hep-2) cancer cell lines. J Photochem Photobiol. 2017; 173: 99-107. Doi: 10.1016/j.jphotobiol.2017.05.031.
38. Dong C, Wu J, Chen Y, Nie J, Chen C. Activation of PI3K/AKT/mTOR pathway causes drug resistance in breast cancer. Frontiers Pharmacol. 2021; 15. Doi Doi:: 10.3389/fphar.2021.628690
39. Veterini L, Savitri AD, Widyaswari MS, Akbar Muhammad R, Fairus A, Zulfikar MQB, Astri M, Ramasima NA, Anggraeni DP, Nainatika RSA, In silico study of the potential of garlic allicin compound as anti-angiogenesis. Trop J Nat Prod Res. 2021; 5(11):1995-1999 DOi:10.26538/tjnpr/v5i11.17
40. Alghuwainem YA, Abd El-Lateef HM, Khalaf MM, Abdelhamid AA, Alfarsi A, Gouda M, Abdelbaset M, Abdou A, Synthesis, structural, DFT, antibacterial, antifungal, anti-inflammatory, and molecular docking analysis of new VO(II), Fe(III), Mn(II), Zn(II), and Ag(I) complexes based on 4-((2-hydroxy-1-naphthyl)azo) benzenesulfonamide. J Mol Liq. 2023; 369(1): 120936. Doi:10.1016/j.molliq.2022.120936.